J. Fluid Mech. (1997), *vol.* 350, *pp.* 331–349. Printed in the United Kingdom

Instability properties of interacting jets

By M. R. GREEN AND D. G. CRIGHTON

Department of Applied Mathematics and Theoretical Physics,
University of Cambridge, Silver Street, Cambridge, CB3 9EW, UK

(Received 22 April 1997 and in revised form 16 July 1997)

Two parallel circular jets, in inviscid incompressible flow, with uniform axial velocity of the same magnitude and direction are placed near to one another, resulting in a strongly coupled field. A given (small) wavenumber in the axial direction is taken and a dispersion relation is found relating the frequency and wavenumber for a given disturbance mode, along with the velocity potentials within and exterior to the jets. The problem is tackled analytically using bipolar coordinates and asymptotic forms for the dispersion relation are found in the small-separation and large-separation limits. Results are then compared with the corresponding two-dimensional problem for plane jets. It is concluded that close-proximity interactions greatly destabilize the varicose mode of the coupled jet, and greatly stabilize the sinuous mode.

1. Introduction

Large-scale coherent structures are thought to play a significant role in noise production and mixing of high-speed jet flows. There have been many studies of such coherent structures from the experimental standpoint, both using signal processing techniques to deduce evidence relating to coherent structures in turbulent flows in 'natural' conditions, and using low levels of external forcing to raise the coherent structures above the background turbulence. From a theoretical standpoint it is natural to approach the modelling of these structures through linear and nonlinear analysis of instability modes developing on the profile of a laminar jet at low speeds and on the mean profile of a turbulent jet at high speeds. Considerable progress has been made in this modelling, using linear and weakly nonlinear analysis, for parallel and weakly diverging flows. Many features remain as yet unaddressed by such instability analyses, but there is much evidence to suggest that such analyses are capable of revealing significant features of the coherent structures in appropriate circumstances.

As an example of the features revealed by instability analysis, we quote the paper by Crighton (1973), who examined the instability modes on a uniform profile of elliptic section, attempting to model the jet used in the Concorde supersonic transport aircraft. Analysis cannot be carried out for the flow conditions appropriate to the Concorde case, but for incompressible inviscid flow, not inappropriate for long-wave modes, the analysis showed that the growth rates of modes corresponding to motion in the plane of the major axis of the ellipse were greatly reduced by ellipticity, while those corresponding to modes in the plane of the minor axis were enhanced, compared with a jet of circular section. Inferences were drawn relating such predictions to the observed noise suppression capabilities of a nozzle producing a jet of elliptic section.

Here we want to address a problem in the same general class, and again one originally motivated by considerations of the Concorde powerplants. In that aircraft,

two engines are mounted under each wing, the two engines under a given wing being placed rather close together, with separation between them of order a jet diameter. The question is whether there are significant hydrodynamic couplings between the coherent structures on the two jets, so that growth rates of one or other possible collective coherent mode might be greatly suppressed by the interaction, and others greatly enhanced. Some evidence of these possibilities was indeed acquired by Rolls-Royce (private communication to Crighton in 1976) in the course of visualization studies of coherent modes on a twin-jet model assembly. These studies were necessarily very restrictive in configuration, but there was nevertheless clear evidence, in shadowgraph and schlieren visualization, of the presence of vigorous large-scale collective motions in which there was manifestly strong interaction between two jets.

Morris (1989) has analysed the case of two parallel jets of circular cross-section, with compressibility effects included and with various models of the mean profiles. His analysis was, however, restricted by its very nature to the case of weak coupling between the jets, in that the separation of the jets was much larger than an instability wavelength. This allowed the basic field of an instability mode on one jet to be expanded in the far field in terms of the natural coordinates of the other, and used as a forcing for modes on that jet, and vice versa. Tam & Seiner (1987) considered the problem of twin supersonic jets also with a weak coupling, in a similar manner. The model showed that kinematically two coupled modes can occur, namely modes symmetric and anti-symmetric with respect to the mid-plane separating the two jets. (In fact, see below, four distinct modes are kinematically possible, and have distinct potentials; but there are only two distinct dispersion relations, corresponding to the modes identified by Tam & Seiner.) Experimentally the symmetric mode has been observed and is fully documented (Seiner, Manning & Ponton 1986), where the question "why has the anti-symmetric mode not been observed?" was posed. The current work may partially answer this question. We offer a different approach, which is restricted in parameter range, but nonetheless capable of revealing the dramatic effects of really close coupling between the jets. We take the case of two geometrically close parallel circular jets, with separation of the same order as a jet radius, in inviscid incompressible flow, with uniform axial velocity of the same magnitude and direction in each of the jets. There are vortex sheet shear layers, of zero thickness, at the jet boundaries, across which one imposes the usual conditions of continuity of pressure and displacement. A given wavenumber in the axial direction is taken, and a dispersion relation is found relating the frequency and wavenumber for a given 'mode', along with a description of the mode shapes within and exterior to the jets. This is achieved by separation of variables in bipolar coordinates. However, to use bipolar coordinates the problem must be two-dimensional in nature, and we therefore have to invoke a long-wave assumption. This is not a severe restriction, because all observations of coherent structures on jets indicate wavelengths at least several times the jet diameter (though the assumption fails when the jets are very close together because then the imaginary part of the wavenumber, giving the spatial growth rate, becomes large). The long-wave approximation leads, then, to Laplace's equation in the variables in a plane normal to the jet axis, with no appearance of the axial wavenumber there. The axial wavenumber does, however, make its appearance, to leading order, in the vortex sheet boundary conditions. It turns out to be unnecessary to go to higher than leading order to obtain significant results.

The 'mode' of collective oscillation of the two jets is specified by an integer n which gives the azimuthal mode number in the bipolar coordinate system onto which the physical jet configuration is mapped. It is only in the separable system that

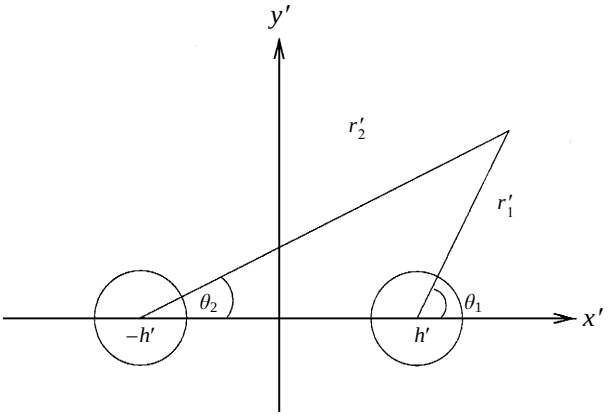

FIGURE 1. Polar coordinates (r_i', θ_i) measured from the jet centres.

one can isolate independent modes, one at a time. In the physical configuration, a given bipolar mode corresponds to a certain distribution of geometrical azimuthal modes on each of the jets. The dispersion relation relates the frequency ω and axial wavenumber k (both possibly complex) and the integer n of a bipolar mode.

Analysis of the dispersion relation reveals two quite different types of behaviour. In one, the jets oscillate symmetrically, in a varicose mode, as it were, in the plane containing their axes, with mirror symmetry in the central plane. In addition, there is also the possibility of symmetry or asymmetry normal to this plane. In the former both jets execute a kind of pinching motion and in the latter a sinuous motion in the direction normal to the plane containing their axes. For these varicose modes we predict that close interaction greatly destabilizes disturbances. In the second type of oscillation, the jets move together in a sinuous oscillation in the plane containing their axes. In the direction normal to that plane the jets may again either execute a symmetric or an anti-symmetric oscillation. For these sinuous modes the effect of close interaction is predicted to be greatly stabilizing.

The corresponding two-dimensional problem is also treated very briefly, and similar results are found. For both the plane jet and circular jet cases, we concentrate on the physically relevant case of spatially growing as opposed to temporally evolving instability waves.

The predictions of this analysis are very specific in qualitative terms, and should be easily capable of confirmation on a suitable low-speed twin-rig jet, through the use of appropriate acoustic forcing with the necessary phase control to produce the required parity and phase of oscillation of the two jets.

2. Two interacting circular jets

We consider the problem of two parallel circular jets of uniform axial velocity u_0 in the positive z'-direction within a fluid of the same density at rest. The flow is incompressible and irrotational, and so there exists a velocity potential ϕ', which satisfies Laplace's equation throughout the fluid, and is determined by imposing the usual conditions of continuity of pressure and displacement across the vortex sheet shear layer at the jet boundaries.

It is assumed that the two jets have centres given by $x' = \pm h'$, $y' = 0$, with radii $r_i' = a_0 + a' f_i(\theta_i)\exp(\mathrm{i}k'z' - \mathrm{i}\omega' t')$, where $a' \ll a_0$ and either the axial wavenumber k'

or frequency ω' is considered as given (a dispersion relation between the two will be derived later). Here (r_i', θ_i) are plane polar coordinates measured from the jet centres, as shown in figure 1, and all primed variables correspond to dimensional quantities. The functions $f_i(\theta_i)$ prescribe the perturbation to the boundary of the jets and will be prescribed later in terms of Fourier components.

It is convenient to define non-dimensional quantities (without primes), where the mean jet radius a_0 and the jet speed u_0 will be used as a characteristic length scale and velocity respectively. Thus set

$$\left.\begin{array}{lll} \phi' = a_0 u_0 \phi, & r_i' = a_0 r_i, & h' = a_0 h, \\ k' = k/a_0, & \omega' = \omega u_0/a_0, & t' = t\, a_0/u_0, \\ a' = a_0 a, & (x', y', z') = a_0(x, y, z), & \end{array}\right\} \tag{2.1}$$

for $i = 1, 2$. The two jets then have centres given by $(x, y) = (\pm h, 0)$, and boundaries

$$r_i = 1 + a f_i(\theta_i) \mathrm{e}^{\mathrm{i}(kz - \omega t)},$$

for $i = 1, 2$, where $a \ll 1$. This form for the boundary of the two jets suggests introducing a reduced potential $\Phi(x, y)$, such that

$$\phi = \mathrm{e}^{\mathrm{i}(kz - \omega t)} \Phi.$$

The potential Φ then satisfies

$$\left(\frac{\partial^2}{\partial x^2} + \frac{\partial^2}{\partial y^2} \right) \Phi = k^2 \Phi. \tag{2.2}$$

Considering only long-wave disturbances ($k' a_0 \equiv k \ll 1$), we may look for an expansion of the form

$$\Phi \sim \Phi_0 + O(k^2), \tag{2.3}$$

so that with error $O(k^2)$, Φ satisfies the two-dimensional Laplace equation everywhere. It is shown in Appendix A, via a formal matching argument, that the form of expansion assumed in (2.3) is the appropriate one, with no terms arising at $O(k)$.

Rather than solve throughout the two-jet region, we consider only the jet in the region $x > 0$ (with boundary $r_1 = 1 + a f_1(\theta_1) \mathrm{e}^{\mathrm{i}(kz - \omega t)}$), and impose a symmetry condition on the plane $x = 0$. We therefore introduce potentials Φ_v and Φ_s such that $\Phi_0 = \Phi_v + \Phi_s$, with $\partial \Phi_v / \partial x = 0$ and $\Phi_s = 0$ on $x = 0$. The even potential Φ_v will be referred to as the varicose mode, and the odd potential Φ_s will be referred to as the sinuous mode. It is convenient to denote the jet region $r_1 < 1$ as V_1 and the jet-free region $r_1 > 1$, $x > 0$ as V_2, and correspondingly for the potentials.

Both Φ_{vi} and Φ_{si} satisfy Laplace's equation

$$\nabla^2 \Phi_{Xi} = 0 \qquad \text{in } V_i, \tag{2.4}$$

for $i = 1, 2$ and X denotes either the varicose or sinuous mode ($X = v, s$). Applying the continuity condition to the displacement of the boundary gives the boundary conditions as

$$\left.\begin{array}{ll} \partial \Phi_{X1} / \partial r_1 = \mathrm{i}a(k - \omega) f_1(\theta_1) & \text{on } r_1 = 1_-, \\ \partial \Phi_{X2} / \partial r_1 = -\mathrm{i}a\omega f_1(\theta_1) & \text{on } r_1 = 1_+, \end{array}\right\} \tag{2.5}$$

for the potentials inside and outside the jet respectively. The symmetry condition is applied on the plane $x = 0$, and takes the form

$$\partial \Phi_{v2} / \partial x = 0, \qquad \Phi_{s2} = 0, \qquad \text{both on } x = 0. \tag{2.6}$$

Finally, to determine the potentials Φ_{vi} and Φ_{si} uniquely it is assumed that Φ_{X1} is regular in the jet region, and that $\Phi_{X2} \to 0$ in the far field.

Once the function $f_1(\theta_1)$ is prescribed, equations (2.4), (2.5) and (2.6) then determine the harmonic functions Φ_{vi} and Φ_{si} everywhere uniquely. However there is also a dynamical condition, which arises from the continuity of pressure across the vortex sheet, and takes the form

$$(k-\omega)\Phi_{X1} = -\omega\Phi_{X2} \qquad \text{on } r_1 = 1. \tag{2.7}$$

When applied to the already fully determined modes (varicose or sinuous), this gives rise to a dispersion relation between non-dimensional wavenumber k and frequency ω.

In general the function $f_1(\theta_1)$ may be described in terms of its Fourier series,

$$f_1(\theta_1) = \sum_{n=0}^{\infty} a_n \cos n\theta_1 + \sum_{n=1}^{\infty} b_n \sin n\theta_1.$$

To aid the clarity of the analysis we consider the even and odd modes in θ_1 separately. Thus for the two types of motion – varicose and sinuous – one must also consider the effect of a perturbation to the jet boundary which is either symmetric or anti-symmetric about the plane $y = 0$, culminating in four possible motions: symmetric varicose, anti-symmetric varicose, symmetric sinuous and anti-symmetric sinuous, as represented schematically in figure 2(*a*). Here the direction of the arrows indicates the displacement at the boundary surface. This becomes clearer if one considers a side view of the two jets, as shown in figure 2(*b*) for the anti-symmetric sinuous and varicose modes. The analysis for all four possible motions is similar, and thus for definiteness we concentrate on a single mode, taken here to be the anti-symmetric sinuous mode. We drop the suffix $X = v, s$ notation, and denote the corresponding potential by Φ_i in the region V_i.

2.1. *The anti-symmetric sinuous mode*

The anti-symmetric sinuous potentials satisfy Laplace's equation

$$\nabla^2\Phi_i = 0 \qquad \text{in regions } V_1 \quad \text{and} \quad V_2, \tag{2.8}$$

and the perturbation function $f_1(\theta_1)$ is taken to have the form of a single odd mode, namely

$$f_1(\theta_1) = \sin m\theta_1, \tag{2.9}$$

where m is a given positive integer. The boundary conditions are then given by

$$\left.\begin{aligned} \partial\Phi_1/\partial r_1 &= \mathrm{i}a(k-\omega)\sin m\theta_1 \qquad \text{on } r_1 = 1_-, \\ \partial\Phi_2/\partial r_1 &= -\mathrm{i}a\omega \sin m\theta_1 \qquad \text{on } r_1 = 1_+, \end{aligned}\right\} \tag{2.10}$$

together with the conditions

$$\left.\begin{aligned} \Phi_2 &= 0 \qquad \text{on } x = 0, \\ \Phi_2 &\to 0 \qquad \text{as } r_1 \to \infty, \end{aligned}\right\} \tag{2.11}$$

and Φ_1 regular in the jet region.

Regarding the (x, y)-plane as the complex Z-plane, the problem can be solved exactly by the method of geometrical inversion. Introducing the conformal mapping

$$\zeta = \xi + \mathrm{i}\eta = 1/(Z + \alpha), \tag{2.12}$$

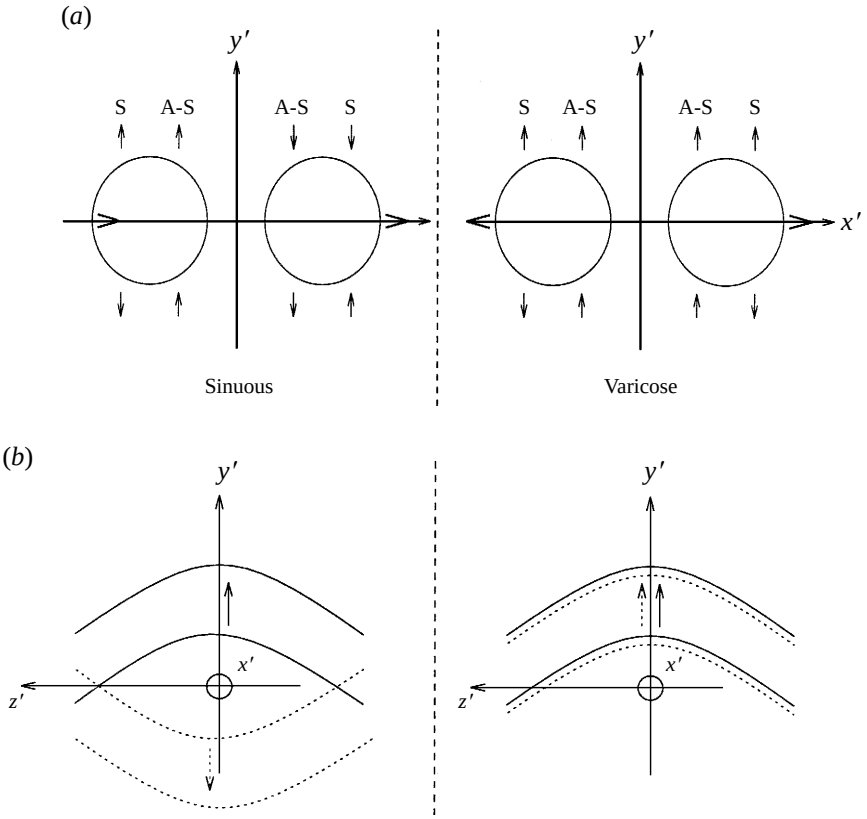

FIGURE 2. (*a*) Symmetric (S) and anti-symmetric (A-S) varicose and sinuous modes. (*b*) Side-view of anti-symmetric sinuous and varicose modes (··· back; — front).

where

$$\alpha = (h^2 - 1)^{1/2}, \tag{2.13}$$

we map the $x = 0$ plane and the jet boundary $r_1 = 1$ onto the respective concentric circles $| \zeta - (2\alpha)^{-1} | = (2\alpha)^{-1}$ and $| \zeta - (2\alpha)^{-1} | = (2\alpha(h + \alpha))^{-1}$ in the ζ-plane, with centres at $(\xi, \eta) = (1/(2\alpha), 0)$ and radii $1/(2\alpha)$ and $1/(2\alpha(h + \alpha))$. Let (σ, λ) represent polar coordinates in the inverted system, based at $(\xi, \eta) = (1/(2\alpha), 0)$, and set

$$\sigma_1 = 1/(2\alpha(h + \alpha)) \qquad \text{and} \qquad \sigma_2 = 1/(2\alpha),$$

as shown in figure 3. The coordinates (σ, λ) are in fact equivalent to the bipolar coordinates that arise when mapping coaxial circles in the (x, y)-plane to concentric circles in the (ξ, η)-plane, under a suitable transformation of curvilinear coordinates (see Morse & Feshbach 1953), and will be referred to as such. Region V_1 now corresponds to $0 < \sigma < \sigma_1$ and region V_2 to $\sigma_1 < \sigma < \sigma_2$, and we continue to use the V_i notation in the ζ-plane.

2.1.1. *Solving for the potential Φ_i in bipolar coordinates*

In terms of bipolar coordinates the problem (2.8) then becomes

$$\nabla^2 \Phi_i = 0 \qquad \text{in } 0 < \sigma < \sigma_1 \text{ and } \sigma_1 < \sigma < \sigma_2, \tag{2.14}$$

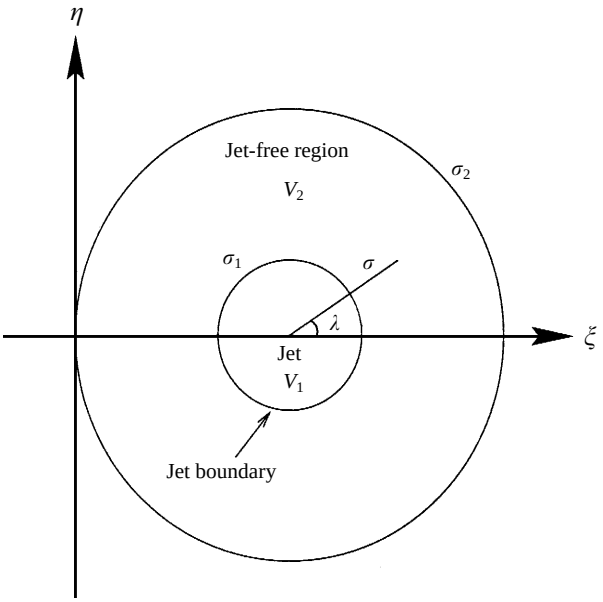

FIGURE 3. Geometry in the ζ-plane.

with Φ_1 regular within V_1. From equation (B 3) in Appendix B, it follows that the perturbation to the jet boundary can be expressed in bipolar coordinates in the form

$$\sin m\theta_1 = -\sum_{q=0}^{m}\sum_{p=0}^{q} {}^{m}C_q\,{}^{m}C_p(-1)^{m-q}(\alpha+h)^{m-p}\frac{\alpha^q}{(h+\cos\lambda)^q}\sin p\lambda. \tag{2.15}$$

The boundary conditions on $r_1 = 1_{\pm}$, given in equation (2.10) above, can then be expressed in terms of bipolar coordinates in the form

$$\left.\begin{aligned}\frac{\partial\Phi_1}{\partial\sigma} &= -2\mathrm{i}a(k-\omega)\alpha^2(h+\alpha)\sum_{q=0}^{m}\sum_{p=0}^{q}\mu_{mpq}\frac{\sin p\lambda}{(h+\cos\lambda)^{q+1}} \quad \text{on } \sigma=\sigma_{1-},\\ \frac{\partial\Phi_2}{\partial\sigma} &= 2\mathrm{i}a\omega\alpha^2(h+\alpha)\sum_{q=0}^{m}\sum_{p=0}^{q}\mu_{mpq}\frac{\sin p\lambda}{(h+\cos\lambda)^{q+1}} \quad \text{on } \sigma=\sigma_{1+},\end{aligned}\right\} \tag{2.16}$$

where

$$\mu_{mpq} = {}^{m}C_q\,{}^{q}C_p(-1)^{m-q}\alpha^q(\alpha+h)^{m-p}. \tag{2.17}$$

The symmetry condition on $x = 0$ is now

$$\Phi_2 = 0 \qquad \text{on } \sigma = \sigma_2 \tag{2.18}$$

with $\Phi_2 \to 0$ as $(\sigma,\lambda) \to (1/(2\alpha),\pi)$ (to satisfy the far-field condition). The consistency condition, arising from continuity of pressure across the vortex sheet, still has the form

$$(k-\omega)\Phi_1 = -\omega\Phi_2, \tag{2.19}$$

but is now applied at $\sigma = \sigma_1 = 1/(2\alpha(h+\alpha))$.

Evidently Φ_1 must be of the form

$$\Phi_1 = \sum_{n=1}^{\infty} A_n \sigma^n \sin n\lambda. \tag{2.20}$$

Applying the boundary condition on $\sigma = \sigma_{1-}$ (equation (2.16)), and inverting the series, gives

$$A_n = \frac{\mathrm{i}a(k-\omega)\alpha(2\alpha(h+\alpha))^n}{n\pi} \sum_{q=0}^{m} \sum_{p=0}^{q} \mu_{mpq} J_{npq}. \tag{2.21}$$

Here the integral J_{npq} is given by

$$J_{npq} = \int_{-\pi}^{\pi} \frac{\sin n\lambda \sin p\lambda}{(h+\cos\lambda)^{q+1}} \mathrm{d}\lambda, \tag{2.22}$$

and is evaluated in Appendix C (equation (C 6)). Thus the anti-symmetric sinuous potential is given in the jet region by

$$\Phi_1 = -\frac{\mathrm{i}a\alpha}{\pi} \sum_{q=0}^{m} \sum_{p=0}^{q} \mu_{mpq} \sum_{n=1}^{\infty} (k-\omega) \left(\frac{2\alpha(h+\alpha)\sigma}{n} \right)^n J_{npq} \sin n\lambda. \tag{2.23}$$

The potential Φ_2 is harmonic in $\sigma_1 < \sigma < \sigma_2$, vanishes on $\sigma = \sigma_2 = 1/(2\alpha)$, and has a normal derivative which is an odd function of λ on $\sigma = \sigma_2$. Therefore the solution in V_2 must be of the form

$$\Phi_2 = \sum_{n=1}^{\infty} A_n \left((2\alpha\sigma)^n - (2\alpha\sigma)^{-n} \right) \sin n\lambda. \tag{2.24}$$

Notice that this automatically satisfies the far-field condition. Applying the boundary condition on $\sigma = \sigma_{1+}$ (equation (2.16) above), and inverting the series, yields

$$A_n = \frac{\mathrm{i}a\omega\alpha(h-\alpha)^n}{\pi n(1+(h-\alpha)^{2n})} \sum_{q=0}^{m} \sum_{p=0}^{q} \mu_{mpq} J_{npq}. \tag{2.25}$$

Thus the anti-symmetric sinuous jet-free-region potential takes the form

$$\Phi_2 = \frac{\mathrm{i}a\alpha}{\pi} \sum_{q=0}^{m} \sum_{p=0}^{q} \mu_{mpq} \sum_{n=1}^{\infty} \frac{\omega(h-\alpha)^n}{n(1+(h-\alpha)^{2n})} J_{npq} \left\{ (2\alpha\sigma)^n - (2\alpha\sigma)^{-n} \right\} \sin n\lambda. \tag{2.26}$$

The consistency condition arising from the continuity of pressure takes the form given in (2.19). Substituting for the potentials Φ_1 and Φ_2 reveals a dispersion relation which relates the non-dimensional wavenumber k to the frequency ω, through the mode number n of a bipolar mode. In fact, despite the apparently complicated nature of the potential solutions, the dispersion relation is found to have the surprisingly simple form

$$(k-\omega)^2 = -\omega^2 \left(\frac{1-(h-\alpha)^{2n}}{1+(h-\alpha)^{2n}} \right), \tag{2.27}$$

where $2h$ is the jet-centre separation and $\alpha = (h^2-1)^{1/2}$.

At first sight it appears surprising that the mode number n of a bipolar mode should arise in the relationship, since this has no physical significance. However it is demonstrated in Appendix B (B 3) that a single mode of perturbation to the jet boundary is necessarily described by all modes (of the same parity) when represented

in terms of bipolar coordinates. This, coupled with the fact that the problem is only separable in bipolar coordinates, implies that a dependence on the bipolar mode number n should be expected. This may be contrasted with the problem of a single jet, where the problem is separable in terms of the Fourier modes themselves, as shown in Appendix D.

2.1.2. *The symmetric sinuous mode*

One may readily repeat all the above analysis for the symmetric sinuous mode, where $f_1(\theta_1) = \cos m\theta_1$. Then it is found that in V_1 the potential takes the form

$$\Phi_1 = \frac{\mathrm{i}a\alpha}{\pi} \sum_{q=0}^{m} \sum_{p=0}^{q} \mu_{mpq} \sum_{n=1}^{\infty} (k-\omega) \frac{(2\alpha(h+\alpha)\sigma)^n}{n} I_{npq} \cos n\lambda, \tag{2.28}$$

and in V_2,

$$\Phi_2 = -\frac{\mathrm{i}a\alpha}{\pi} \sum_{q=0}^{m} \sum_{p=0}^{q} \mu_{mpq} \sum_{n=1}^{\infty} \frac{\omega(h-\alpha)^n}{n(1+(h-\alpha)^{2n})} I_{npq} \{(2\alpha\sigma)^n - (2\alpha\sigma)^{-n}\} \cos n\lambda, \tag{2.29}$$

with μ_{mpq} as in equation (2.17). Here the integral I_{npq} is given by

$$I_{npq} = \tfrac{1}{2}\mathrm{Re}\left(\int_{-\pi}^{\pi} \frac{\cos n\lambda \cos p\lambda}{(h+\cos\lambda)^{q+1}} \mathrm{d}\lambda \right), \tag{2.30}$$

and is evaluated in (C 5). Applying the vortex sheet condition on the surface $\sigma = \sigma_1$, it is found that the symmetric sinuous mode must also satisfy the dispersion relation (2.27) above. That is, symmetry about the $y = 0$ plane does not affect the dispersion relation, even though the potentials are somewhat different in nature.

2.2. *The varicose mode*

Following the same procedure one can determine the varicose modes (symmetric and anti-symmetric). It is found that the symmetric varicose potential is given by

$$\left.\begin{aligned} \Phi_1 &= C_0 + \frac{\mathrm{i}a\alpha}{\pi} \sum_{q=0}^{m} \sum_{p=0}^{q} \mu_{mpq} \sum_{n=1}^{\infty} \frac{(k-\omega)(2\alpha(h+\alpha))^n}{n} I_{npq} \cos n\lambda, \\ \Phi_2 &= \frac{\mathrm{i}a\alpha}{\pi} \sum_{q=0}^{m} \sum_{p=0}^{q} \mu_{mpq} \sum_{n=1}^{\infty} \frac{\omega(h-\alpha)^n}{n(1-(h-\alpha)^{2n})} I_{npq} \{(2\alpha\sigma)^n + (2\alpha\sigma)^{-n}\} \cos n\lambda \\ &\quad -\frac{2\mathrm{i}a\alpha}{\pi} \sum_{q=0}^{m} \sum_{p=0}^{q} \mu_{mpq} \sum_{n=1}^{\infty} \frac{\omega(h-\alpha)^n(-1)^n}{n(1-(h-\alpha)^{2n})} I_{npq}, \end{aligned}\right\} \tag{2.31}$$

and the anti-symmetric varicose potential by

$$\left.\begin{aligned} \Phi_1 &= -\frac{\mathrm{i}a\alpha}{\pi} \sum_{q=0}^{m} \sum_{p=0}^{q} \mu_{mpq} \sum_{n=1}^{\infty} \frac{(k-\omega)(2\alpha(h+\alpha))^n}{n} J_{npq} \sin n\lambda, \\ \Phi_2 &= -\frac{\mathrm{i}a\alpha}{\pi} \sum_{q=0}^{m} \sum_{p=0}^{q} \mu_{mpq} \sum_{n=1}^{\infty} \frac{\omega(h-\alpha)^n}{n(1-(h-\alpha)^{2n})} J_{npq} \{(2\alpha\sigma)^n + (2\alpha\sigma)^{-n}\} \sin n\lambda. \end{aligned}\right\} \tag{2.32}$$

Here C_0 is a constant term. Applying the vortex sheet pressure condition it follows that

$$C_0 = \frac{2\mathrm{i}a\alpha}{\pi} \sum_{n=1}^{\infty} \frac{(-1)^n \omega^2 (h-\alpha)^n}{(k-\omega)^2(1-(h-\alpha)^{2n})} \sum_{q=0}^{m} \sum_{p=0}^{q} \mu_{mpq} I_{npq}, \tag{2.33}$$

from the $n = 0$ term, and both modes must satisfy the dispersion relation

$$(k-\omega)^2 = -\omega^2 \left(\frac{1+(h-\alpha)^{2n}}{1-(h-\alpha)^{2n}} \right), \tag{2.34}$$

for $n = 1, 2, 3, \ldots$. The dispersion relation (2.34) should be compared with that in equation (2.27) for the sinuous modes, and it is readily seen that the n-dependent factors on the right-hand sides are the reciprocals of each other. Again it is noted that the non-dimensional wavenumber k and frequency ω are related through the bipolar mode number n.

2.3. *Stability analysis*

Introducing

$$\Gamma_s = \frac{1-(h-\alpha)^{2n}}{1+(h-\alpha)^{2n}}, \qquad \Gamma_v = \frac{1+(h-\alpha)^{2n}}{1-(h-\alpha)^{2n}}, \tag{2.35}$$

the dispersion relations (2.27) and (2.34) may be cast in the single form

$$(k-\omega)^2 = -\omega^2 \Gamma_X, \tag{2.36}$$

where $X = s, v$ and relates to sinuous or varicose respectively, and we note that

$$\Gamma_v > 1 > \Gamma_s. \tag{2.37}$$

For a given real frequency (2.36) may be solved for wavenumber k (complex in general) in the form

$$k = \omega(1 \pm \mathrm{i}(\Gamma_X)^{1/2}), \tag{2.38}$$

and thus the spatial growth rate of the instability is given by $\omega(\Gamma_X)^{1/2}$. It is shown in Appendix D that for a single jet the growth rate of instability is given by ω (for long waves). Therefore the inequality (2.37) implies that the effect of placing two jets together enhances the instability of the varicose mode but stabilizes the sinuous mode, when compared with the single-jet result. But when the jets are far apart ($h \gg 1$), it follows that

$$\Gamma_X \sim 1 \qquad \text{and} \qquad (k-\omega)^2 \sim -\omega^2, \tag{2.39}$$

which is the expected result for a single jet with small wavenumber (equation (D 7) in Appendix D).

It is more interesting to examine the behaviour when the jets are very close together; thus, introducing a parameter μ, with $h = \cosh\mu$ and $\alpha = \sinh\mu$, Γ_s and Γ_v are then given by

$$\Gamma_s = \tanh n\mu, \qquad \Gamma_v = \coth n\mu. \tag{2.40}$$

If we set $h = 1 + \delta$, with $\delta \ll 1$, so that the two jets are very close, it follows that $\mu = (2\delta)^{1/2}$, and for bipolar modes with $n \ll 1/(2\delta)^{1/2}$ that

$$\Gamma_s \sim n(2\delta)^{1/2}, \qquad \Gamma_v \sim \frac{1}{n(2\delta)^{1/2}}. \tag{2.41}$$

Therefore, the varicose modes (with $n \ll 1/(2\delta)^{1/2}$) are greatly destabilized, whereas the sinuous modes are almost completely stabilized. For mode numbers with $n \gg 1/(2\delta)^{1/2}$, $\coth n\mu \sim \tanh n\mu \sim 1$, and we recover the single-jet result, as given above in equation (2.39). That is, it is only the lower modes that 'feel' the presence of the other jet.

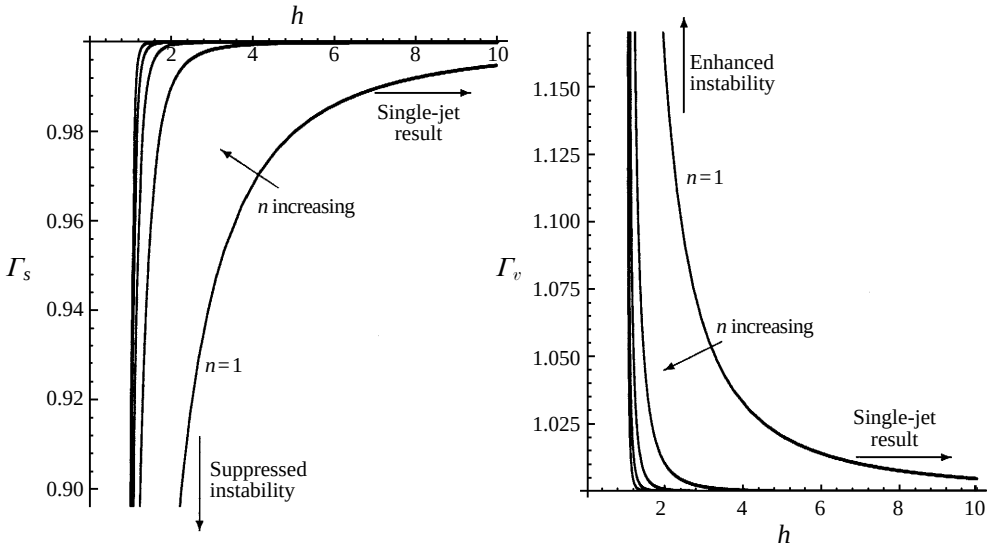

FIGURE 4. Instability growth rate factors $\Gamma_s(h)$ and $\Gamma_v(h)$ for modes $n = 1, 2, 3, 4, 5$.

This may be explained geometrically if one considers the effect of setting $h = 1+\delta$, with $\delta \ll 1$, in the bipolar coordinate plane. Then we find that $\sigma_1 \sim \sigma_2 \sim 1/(2(2\delta)^{1/2})$, so that both the jet region and jet-free region become large. However the difference between their radii is finite,

$$\sigma_2 - \sigma_1 \sim \tfrac{1}{2} \qquad \text{for } \delta \ll 1. \tag{2.42}$$

The wavelength λ_n of the nth bipolar mode, on the jet surface is given by

$$\lambda_n \sim \frac{\pi}{n(2\delta)^{1/2}}. \tag{2.43}$$

Notice that when

$$\lambda_n \gg 1/2, \quad \text{i.e.} \quad n(2\delta)^{1/2} \ll 2\pi, \tag{2.44}$$

the wavelength of the nth bipolar mode is much larger than the separation of the jet surface $\sigma = \sigma_1$ from the 'wall region' $\sigma = \sigma_2$ and we have a strong interaction between the two jets, as expected. Conversely, when the wavelength is much smaller than the separation, the modes do not see the 'wall region' and there is no interaction. Figure 4 shows a plot of the factors Γ_s and Γ_v for the first five bipolar modes, against separation function h. As h increases, we approach the single-jet result, as predicted. It is clearly seen that suppression or enhancement of instability becomes more noticeable for small values of h, with dominant contributions coming from the lower mode numbers. However, within the varicose mode growth rate, there is a restriction on how small $h-1$ can become, due to the long-wave assumption. In fact the condition $k \ll 1$ requires $\omega\Gamma_v^{1/2} \ll 1$, so that

$$\omega^2 \ll n(2\delta)^{1/2} \ll 2\pi \tag{2.45}$$

is required, if the varicose growth rate is to remain finite as $h \to 1$. There is no such restriction on the sinuous mode growth rate. This suggests that when the jets 'closeness' is $O(\omega^4)$ a more thorough analysis of the varicose growth rate would be required and this is simply impossible as the three-dimensional Laplacian is not

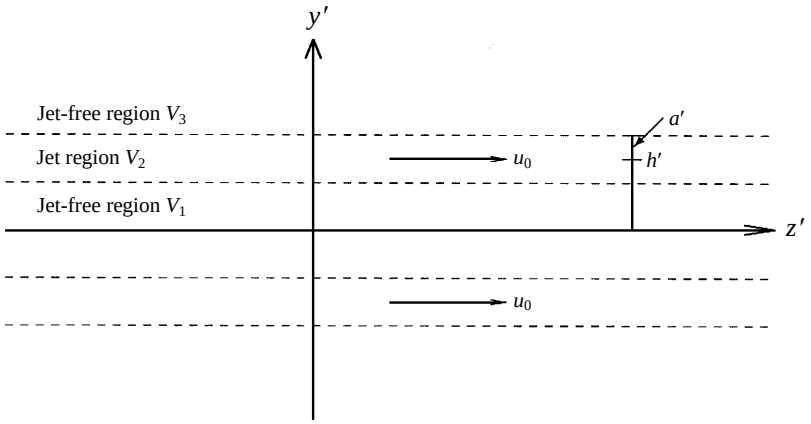

FIGURE 5. Two interacting plane jets.

separable in cylindrical bipolar coordinates. With this in mind we therefore now consider the analogous two-dimensional problem of a pair of plane parallel jets.

3. Two interacting plane jets

Consider the two-dimensional problem analogous to that studied in §2, so that the jet motion is in the (y', z')-plane. It is assumed that we have a pair of plane jets of constant velocity u_0 in the positive z'-direction, where the mid-point of the two jets has separation $2h'$ and each jet is of width $2a'$, as shown in figure 5.

Without loss of generality we may assume that the jet boundaries are given by

$$y' = \pm(h' + a' + a'_2 e^{i(k'z' - \omega' t')}), \qquad y' = \pm(h' - a' + a'_1 e^{i(k'z' - \omega' t')}) \tag{3.1}$$

where k' and ω' are the wavenumber and frequency, as before, and $a'_i \ll a'$, for $i = 1, 2$. As with the case of circular jets, we may impose a symmetry condition on $y' = 0$, and solve for a single jet in $y' > 0$ in the form of a varicose mode (with potential ϕ'_v satisfying $\partial\phi'_v/\partial y' = 0$ on $y' = 0$) and a sinuous mode (with potential ϕ'_s satisfying $\phi'_s = 0$ on $y' = 0$). The problem may be non-dimensionalized in a similar manner to §2 where the jet half-width a' is used as a characteristic length scale. The jet boundaries are then given by

$$y = h + 1 + a_2 e^{i(kz - \omega t)}, \qquad y = h - 1 + a_1 e^{i(kz - \omega t)}, \tag{3.2}$$

where $h \geqslant 1$, and $a_i = a'_i/a' \ll 1$. The flow is incompressible everywhere and so the potentials ϕ_X, $X = v, s$, are harmonic functions. Thus introducing the reduced potentials $\Phi_X(y)$, related to the total potential $\phi_X(y, z, t)$ by

$$\phi_X(y, z, t) = \Phi_X(y) e^{i(kz - \omega t)},$$

it follows that

$$\left(\frac{\partial^2}{\partial y^2} - k^2\right) \Phi_X = 0 \qquad \text{for } y > 0. \tag{3.3}$$

Applying the vortex sheet boundary conditions on the jet surfaces leads to two equations involving arbitrary a_1 and a_2, and it follows that the varicose mode satisfies

the dispersion relation

$$(k-\omega)^4+\omega^2(k-\omega)^2\coth 2k\left(\coth k(h-1)+\frac{k}{|k|}\right)+\frac{\omega^4 k}{|k|}\coth k(h-1)=0, \quad (3.4)$$

and the sinuous mode satisfies

$$(k-\omega)^4+\omega^2(k-\omega)^2\coth 2k\left(\tanh k(h-1)+\frac{k}{|k|}\right)+\frac{\omega^4 k}{|k|}\tanh k(h-1)=0. \quad (3.5)$$

The possibility of complex k is allowed in these equations by the understanding that $|k|$ is to be interpreted as $k\,\mathrm{sgn}(\mathrm{Re}(k))$. If we consider the limit $h\to 1$, so that the two jets meet and become one, the dispersion relations above reduce to

$$(k-\omega)^2\coth|2k|=-\omega^2 \qquad \text{and} \qquad (k-\omega)^2\tanh|2k|=-\omega^2, \quad (3.6)$$

which are the dispersion relations associated with the respective varicose and sinuous modes of a single jet of half-width 2 (Crighton 1992). The above analysis is valid for all wavenumbers k, but to compare the results with the circular-jet problem of §2 we seek the long-wave approximation ($k\ll 1$) to the dispersion relations (3.4) and (3.5) above. We consider the limit $k\ll 1$ in the varicose dispersion relation (3.4), and look for the possibility of a mode with $k\sim\omega^\beta$ for some $\beta<1$ (so that $k\gg\omega$). Then it follows that $\beta=1/2$, and that

$$k\sim\frac{\omega^{1/2}}{(2(h-1))^{1/4}}\mathrm{e}^{\mathrm{i}\pi(2n+1)/4}, \quad (3.7)$$

for $n=0,1,2,3$. Thus for $h-1$ of order unity and $k,\omega\ll 1$, the varicose mode grows like $\omega^{1/2}$. Note that for $h-1\sim O(\omega^2)$, k in equation (3.7) becomes an order-one quantity and a more thorough analysis is required to take account of the non-uniformity associated with (3.7). If one then writes $h-1\sim C\omega^2$, it follows that

$$k\sim\omega\left(1\pm\mathrm{i}\,|\omega|^{1/2}\right), \quad (3.8)$$

so that the growth rate is now proportional to $\omega^{3/2}$, and is not singular as is suggested by (3.7). The result (3.8) is the long-wave limit associated with the varicose mode dispersion relation of a single jet, as given in equation (3.6) above, which may be expected to arise when the jets are near to one another.

Proceeding in a similar manner for the sinuous mode with $k\ll 1$, it follows that the dominant mode is given by

$$k\sim\left(\frac{\omega}{4}\right)^{2/3}\left(-1\pm\mathrm{i}\,3^{1/3}\right), \quad (3.9)$$

for all values of h (assuming $k(h-1)\ll 1$, as usual). This is the expected result for the long-wave limit of the sinuous mode of a single jet as given above in equation (3.6). That is, even when h is of order unity, the jet separation does not affect the dispersion relation for a single jet, quite unlike the varicose mode result given in equation (3.7).

It therefore appears that for separations $h-1$ of order unity, the varicose mode has the dominant growth rate ($\omega^{1/2}$ as opposed to the $\omega^{2/3}$ of the sinuous mode), which is analogous to the results of §2 for two parallel circular jets. However, when the jets are brought very close together, the sinuous mode retains the growth rate proportional to $\omega^{2/3}$, whereas the varicose mode growth rate is reduced significantly to the single-jet result of $O(\omega^{3/2})$. These results should be compared with those of the circular jets and in particular the apparent singularity that arises in the varicose mode growth rate as

$h \to 1$; and this suggests that to avoid the singularity in the varicose mode a more thorough analysis of the full three-dimensional problem is necessary. Unfortunately this is permanently beyond reach, other than through numerical studies.

4. Conclusion

The problem of the instability of two circular jets of uniform velocity is, in general, too difficult to solve analytically, using existing techniques. Instead previous work has generally concentrated on a numerical approach (see Morris 1989) with analytical results given only for the case of weakly interacting jets, where the separation is larger than a typical wavelength of the medium. We have opted for a different approach, which is more restrictive in parameter range, by considering only long-wave perturbations. As mentioned previously, this is not as restrictive as it may first seem, because all observations of coherent structures on jets indicate wavelengths at least several times the jet diameter. Also this analysis has the added effect of permitting a strong coupling between the two jets, where they are geometrically close (i.e. well within an axial wavelength of one another), which was necessarily absent from previous work in the area. By invoking the long-wave approximation the problem may be solved exactly by using a conformal transformation (or equivalently bipolar coordinates). The solution may be decomposed into a varicose and a sinuous mode with additional symmetry properties about the plane $y = 0$. The potentials are, in general, very complicated functions, given in the form of infinite series in bipolar coordinates (equations (2.23) *et seq.*). However the resulting dispersion relation has the surprisingly simple form

$$(k - \omega)^2 = -\omega^2 \Gamma_X, \tag{4.1}$$

where

$$\Gamma_s = \frac{1 - (h - \alpha)^{2n}}{1 + (h - \alpha)^{2n}}, \qquad \Gamma_v = \frac{1 + (h - \alpha)^{2n}}{1 - (h - \alpha)^{2n}}, \tag{4.2}$$

and the suffices refer to sinuous and varicose as usual. The parity about the plane $y' = 0$ does not affect the form of the dispersion relation; it is only the parity about the plane $x' = 0$ which matters (though parity about the plane $y' = 0$ does affect the form of the potentials in a significant way).

The key results of the paper are (4.1) and (4.2) above, and it is noted that the bipolar mode number arises naturally within the dispersion relations. This reflects the fact that a single physical perturbation mode $e^{im\theta_1}$ corresponds to an infinite number of bipolar 'unphysical' modes, but the problem is only separable in the latter coordinates. On analysing the stability of the various modes it was shown that the presence of the second jet greatly enhances the spatial-instability growth rate of the varicose mode and suppresses the sinuous growth rate, when compared with the results for a single jet. This provides a possible answer to the question posed by Tam & Seiner (1987), as to why the varicose mode and not the sinuous mode has been observed experimentally. Indeed the current work suggests that it is not the subsonic or supersonic nature of the jets that is responsible for the observed effects, but rather inertial instability and a particular geometrical configuration. The effect of the change in growth rates increases as the jets are brought closer together, and indeed it appears that the varicose mode is arbitrarily rapidly amplified when the jets are very close together, while the sinuous mode is arbitrarily slowly amplified. However a comparison with the analogous two-dimensional plane problem suggests that the singularity in the varicose growth rate must be limited due to a restriction on

how small $h-1$ can become. For plane jets it was found, for separations of the jets of order unity, that the varicose mode again dominates the sinuous mode instability growth rate. However when the two jets are close together there is a boundary layer effect in the dispersion relation for the varicose mode, and the results obtained for separation of order unity are not uniformly valid. When this is analysed in more detail, it is found that as the plane jets become very close (separation $O(\omega^2)$) the varicose growth rate is significantly reduced and now the sinuous mode dominates. The circular jets results therefore may suggest a similar type of boundary layer effect arising for separation $O(\omega^4)$, and this is likely to require a complete analysis of the full three-dimensional dispersion relation, which is, unfortunately, permanently beyond the scope of analysis. However for reasonable values of $h-1$ ($\gg \omega^2$ for plane jets, and $\gg \omega^4$ for circular jets), both models predict the varicose mode as having the dominant growth rate. In fact the circular jets have to be much closer to one another, separation $O(\omega^4)$, than the plane jets, separation $O(\omega^2)$, before the singularity in the growth rate is reached. One reason for this must be the difference in geometry for small separations. As the two circular jets are brought closer together, they meet along a line of contact as opposed to the planar case where the jets meet at a plane of contact. It could also be argued that, when the jets become too close the model is inappropriate as it stands, and one should include additional effects such as viscosity if a physically realizable conclusion is to be obtained. Finally it is interesting to note that for reasonable values of the separation both plane and circular jet varicose growth rates have a similar dependence on $h-1$, in the form $(h-1)^{-1/4}$, but the planar case is more unstable with growth $O(\omega^{1/2})$, compared with $O(\omega)$ for the circular case.

Support for the DAMTP programme in acoustics, structural dynamics and wave theory provided by the US Office of Naval Research (Dr G. L. Main) is gratefully acknowledged.

Appendix A. A matching problem in potential theory

Here we demonstrate the correctness of assuming an expansion of the form $\Phi \sim \Phi_0 + O(k^2)$, and in particular ignoring eigensolutions of $O(k)$, in the twin-jet problem of §2, via a formal matching argument. Using the axial wavenumber k as a small expansion parameter gives rise to a singular perturbation problem where the inner field (with inner potential Φ) must be matched to an outer field (χ say) which has variables scaled on the wavelength of the perturbation. If (x, y) are inner variables scaled on the jet radius then we define outer variables by (X, Y), so that

$$(x, y) = k^{-1}(X, Y) \qquad \text{with } k \ll 1, \tag{A 1}$$

and

$$\Phi(x, y, k) = \chi(X, Y, k).$$

The two solutions Φ and χ may then be matched accordingly using Van Dyke's (1975) matching principle,

$$\Phi^{(m,n)} = \chi^{(n,m)}, \tag{A 2}$$

for all integers m, n, in the notation of Crighton & Leppington (1973) and Van Dyke (1975).

We proceed by looking for an inner expansion of the form $\Phi \sim \Phi_0 + k\Phi_1$. The potential Φ_0 was determined in §2. Ultimately it is the far-field behaviour of the inner

solution that is necessary for matching,

$$\Phi_0 = A\frac{\cos\theta}{r} + B\frac{\sin\theta}{r} + O(1/r^2) \qquad \text{for } r \gg 1. \tag{A 3}$$

Here (r, θ) are plane polar coordinates measured from the origin of the (x, y)-plane, $(r^2 = x^2 + y^2, \quad \theta = \arctan(y/x))$, and A and B are given by

$$\left.\begin{aligned} A &= \frac{4\mathrm{i}a\alpha^2}{\pi}\sum_{q=0}^{m}\sum_{p=0}^{q}\mu_{mpq}\sum_{n=1}^{\infty}\left(\frac{\omega(\alpha-h)^n}{1+(h-\alpha)^{2n}}I_{npq}\right), \\ B &= -\frac{4\mathrm{i}a\alpha^2}{\pi}\sum_{q=0}^{m}\sum_{p=0}^{q}\mu_{mpq}\sum_{n=1}^{\infty}\left(\frac{\omega(\alpha-h)^n}{1-(h-\alpha)^{2n}}J_{npq}\right), \end{aligned}\right\} \tag{A 4}$$

and arise from the symmetric sinuous and anti-symmetric varicose modes, respectively. Therefore, the leading-order inner potential is $O(k)$ in the far field and from the matching principle (A 2) the leading-order outer field χ must also be $O(k)$.

Substituting the expansion for Φ_0 into equations (2.2), (2.5)–(2.7), the potential Φ_1 is harmonic, with zero normal derivative on $r_1 = 1$, and zero normal derivative or zero potential on $x = 0$ (symmetry condition). In addition, since Φ_0 is $O(k)$ in the far field, it follows (see Crighton & Leppington 1973) that Φ_1 can only be $O(1)$ in the far field. In the bipolar coordinate system, Φ_1 is harmonic in $0 < \sigma < \sigma_2$, with $\partial\Phi_1/\partial\sigma = 0$, on $\sigma = \sigma_1$, and $\partial\Phi_1/\partial\sigma = 0$ or $\Phi_1 = 0$, on $\sigma = \sigma_2$. The far-field condition also requires $\Phi_1 = O(1)$ as $(\lambda, \sigma) \to (1/(2\alpha), \pi)$. It transpires that the only possibility is

$$\Phi_1 = C_0, \quad \text{for } \sigma < \sigma_1, \qquad \text{and} \quad \Phi_1 = D_0, \quad \text{for } \sigma_1 < \sigma < \sigma_2, \tag{A 5}$$

where C_0 and D_0 are constants related via the vortex sheet boundary condition on $\sigma = \sigma_1$,

$$(k - \omega)C_0 = -\omega D_0.$$

The constant D_0 holds in the jet-free region, and thus in the far field, and so may be determined by matching with an outer solution. Thus to $O(k)$ the inner potential Φ has the far-field form

$$\Phi^{(1)} = (A\cos\theta + B\sin\theta)/r + kD_0 \qquad \text{for } r \gg 1, \tag{A 6}$$

in terms of the inner variables (r, θ).

The leading outer potential χ satisfies the modified Bessel equation

$$(\nabla^2 - 1)\chi(R, \theta) = 0. \tag{A 7}$$

In terms of outer coordinates the geometry of the jets no longer appears and the boundary conditions are now replaced with an equivalent matching condition. Substituting for $r = R/k$ in equation (A 6), it follows that

$$\Phi^{(1,1)} = k\left((A\cos\theta + B\sin\theta)/R + D_0\right). \tag{A 8}$$

Applying the matching condition (A 2) with $m = n = 1$, and using the fact that χ satisfies the modified Bessel equation, it follows that

$$\chi \sim k\,(q_1\cos\theta + q_2\sin\theta)\,K_1(R) + O(k^2), \tag{A 9}$$

and that

$$\chi^{(1,1)} = (q_1\cos\theta + q_2\sin\theta)/r. \tag{A 10}$$

Equating (A 8) to (A 10) determines all the coefficients in the form

$$D_0 = 0, \qquad q_1 = A, \qquad \text{and} \qquad q_2 = B. \tag{A 11}$$

Thus to leading order the outer potential χ is given by

$$\chi \sim k(A\cos\theta + B\sin\theta)K_1(R), \tag{A 12}$$

and there is no term at $O(k)$ in the inner expansion (since $D_0 = 0 \Rightarrow C_0 = 0 \Rightarrow \Phi_1 = 0$).

Appendix B. Expansion of a single mode of the form $e^{im\theta_1}$ in bipolar coordinates

In order to evaluate the integrals I_{npq} and J_{npq} in §2, it is necessary to expand $e^{im\theta_1}$ in terms of coordinates (σ, λ), evaluated on $\sigma = \sigma_1$ (corresponding to $r_1 = 1$). From equation (2.12) it follows that

$$e^{i\theta_1} = Z - h = \frac{1}{\zeta} - (\alpha + h),$$

and hence

$$e^{im\theta_1} = \sum_{q=0}^{m} {}^{m}C_q \left(\frac{1}{\zeta}\right)^q (-1)^{m-q}(\alpha + h)^{m-q}, \tag{B 1}$$

where ${}^{m}C_q$ are the usual binomial coefficients. On $\sigma = \sigma_1$,

$$\frac{1}{\zeta} = \frac{\alpha(h + \alpha + e^{-i\lambda})}{h + \cos\lambda}$$

and applying the binomial expansion again, it is found that

$$\left(\frac{1}{\zeta}\right)^q = \frac{\alpha^q}{(h + \cos\lambda)^q} \sum_{p=0}^{q} {}^{q}C_p\,(h + \alpha)^{q-p} e^{-ip\lambda}. \tag{B 2}$$

We keep the factor $1/(h + \cos\lambda)^q$ in its unexpanded form since this arises naturally in the integrals I_{npq} and J_{npq}, in equations (2.30) and (2.22). Combining (B 1) and (B 2) reveals that a single Fourier mode on $r_1 = 1$ takes the form

$$e^{im\theta_1} = \sum_{q=0}^{m}\sum_{p=0}^{q} {}^{m}C_q\,{}^{q}C_p(-1)^{m-q}(\alpha + h)^{m-p}\frac{\alpha^q}{(h + \cos\lambda)^q} e^{-ip\lambda}. \tag{B 3}$$

If we were to expand the denominator further, it follows that a single mode in the physical plane actually corresponds to an infinite number of bipolar modes.

Appendix C. Evaluation of the integrals I_{npq} and J_{npq}

In order to determine the coefficients of the potential Φ_0 in §2 it is necessary to calculate integrals of the form

$$I_{npq} = \int_{-\pi}^{\pi} \frac{\cos n\lambda \cos p\lambda}{(h + \cos\lambda)^{q+1}} d\lambda, \tag{C 1}$$

and

$$J_{npq} = \int_{-\pi}^{\pi} \frac{\sin n\lambda \sin p\lambda}{(h + \cos\lambda)^{q+1}} d\lambda. \tag{C 2}$$

Consider, for definiteness, (C 1). Introducing $N = n + p$ and $M = |n - p|$, (C 1) may be re-written as

$$I_{npq} = \tfrac{1}{2}\mathrm{Re}\left(\int_{-\pi}^{\pi} \frac{\mathrm{e}^{\mathrm{i}N\lambda} + \mathrm{e}^{\mathrm{i}M\lambda}}{(h + \cos\lambda)^{q+1}}\mathrm{d}\lambda\right). \tag{C 3}$$

Writing $z = \mathrm{e}^{\mathrm{i}\lambda}$ reduces this to an integral around the unit circle c, in the form

$$I_{npq} = -\tfrac{1}{2}\mathrm{Re}\left(2^{q+1}\mathrm{i}\oint_c \frac{z^{N+q} + z^{M+q}}{(z - z_+)^{q+1}(z - z_-)^{q+1}}\mathrm{d}z\right), \tag{C 4}$$

where

$$z_+ = \alpha - h, \qquad z_- = -(\alpha + h),$$

and $\alpha = (h^2 - 1)^{1/2}$ as before. Thus only the pole at $z = z_+$ contributes to (C 4). Applying Cauchy's Residue Theorem gives

$$\begin{aligned} I_{npq} = {} & \frac{\pi}{\alpha^{q+1}} \sum_{r=0}^{q} {}^{n+p+q}C_{q-r}\,{}^{q+r}C_q (-1)^r \frac{(\alpha - h)^{n+p+r}}{(2\alpha)^r} \\ & + \frac{\pi}{\alpha^{q+1}} \sum_{r=0}^{q} {}^{|n-p|+q}C_{q-r}\,{}^{q+r}C_q (-1)^r \frac{(\alpha - h)^{|n-p|+r}}{(2\alpha)^r}, \end{aligned} \tag{C 5}$$

The integral J_{npq} may be evaluated in a similar manner, and it is found that

$$\begin{aligned} J_{npq} = {} & \frac{\pi}{\alpha^{q+1}} \sum_{r=0}^{q} {}^{|n-p|+q}C_{q-r}\,{}^{q+r}C_q (-1)^r \frac{(\alpha - h)^{|n-p|+r}}{(2\alpha)^r} \\ & - \frac{\pi}{\alpha^{q+1}} \sum_{r=0}^{q} {}^{n+p+q}C_{q-r}\,{}^{q+r}C_q (-1)^r \frac{(\alpha - h)^{n+p+r}}{(2\alpha)^r}. \end{aligned} \tag{C 6}$$

Appendix D. Single circular jet

For completeness we give the solution for a single circular jet of uniform axial velocity u_0. It is assumed that the jet boundary may be described in a similar manner to that of §2, so that the free surface has the form $r = 1 + af(\theta)\mathrm{e}^{\mathrm{i}(kz - \omega t)}$. Here (r, θ) are plane polar coordinates measured from the centre of the jet and all variables have been non-dimensionalized as before. The function $f(\theta)$ is taken as a single mode $\mathrm{e}^{\mathrm{i}m\theta}$ and we may then introduce the reduced potential Φ, related to the full potential ϕ via

$$\phi(r, \theta, z, t) = \Phi(r)\mathrm{e}^{\mathrm{i}(kz - \omega t + m\theta)}. \tag{D 1}$$

Following the procedure adopted in §2, the reduced potential satisfies

$$r^2\frac{\partial^2\Phi}{\partial r^2} + r\frac{\partial\Phi}{\partial r} - \left(k^2r^2 + m^2\right)\Phi = 0 \tag{D 2}$$

throughout the entire region, and must satisfy the boundary conditions

$$\frac{\partial\Phi}{\partial r} = \mathrm{i}a(k - \omega), \qquad \frac{\partial\Phi}{\partial r} = -\mathrm{i}a\omega, \tag{D 3}$$

on $r = 1_-$ and $r = 1_+$, respectively. If we denote the jet region ($r < 1$) by V_1, with corresponding potential Φ_1, and the jet-free region by V_2, with corresponding potential Φ_2, it is easily shown that

$$\Phi_1 = \frac{\mathrm{i}a(k - \omega)}{|k|\,K_m'(|k|)}K_m(|k|\,r) \qquad \text{and} \qquad \Phi_2 = -\frac{\mathrm{i}a\omega}{|k|\,I_m'(|k|)}I_m(|k|\,r). \tag{D 4}$$

Here $K_m(x)$ and $I_m(x)$ are modified Bessel functions of integer order which are respectively bounded at infinity and regular at the origin. There is also the vortex sheet pressure condition on the jet boundary,

$$(k-\omega)\Phi_1 = -\omega\Phi_2 \qquad \text{on } r = 1, \tag{D 5}$$

and this leads to a dispersion relation relating k and ω in the form

$$(k-\omega)^2 = \omega^2 \frac{K_m'(|k|)}{K_m(|k|)} \frac{I_m(|k|)}{I_m'(|k|)}. \tag{D 6}$$

In order to compare results with the twin-jet problem in §2 we need the long-wave limit of equation (D 6) above, and we find

$$(k-\omega)^2 \sim -\omega^2 \qquad \text{for } k \ll 1. \tag{D 7}$$

That is, the long-wave limit for a circular jet of constant strength actually gives rise to the dispersion relation for a plane vortex sheet of constant strength. In the above complex k is catered for by the convention $|k| = \operatorname{sgn}(\mathrm{Re}(k))$.

REFERENCES

Crighton, D. G. 1973 Instability of an elliptic jet. *J. Fluid Mech.* **59**, 665–672.

Crighton, D. G. 1992 The jet edge-tone feedback cycle; linear theory for the operating stages. *J. Fluid Mech.* **234**, 361–391.

Crighton, D. G. & Leppington, F. G. 1973 Singular perturbation methods in acoustics: diffraction by a plate of finite thickness. *Proc. R. Soc. Lond.* A **335**, 313–339.

Morris, P. J. 1989 The resonance of twin supersonic jets. *AIAA Paper* 89-1089.

Morse, P. M. & Feshbach, H. 1953 *Methods of Theoretical Physics.* McGraw-Hill.

Seiner, J. M., Manning, J. C. & Ponton, M. K. 1986 Dynamic pressure loads associated with twin supersonic plume resonance. *AIAA Paper* 86-1539.

Tam, C. K. W. & Seiner, J. M. 1987 Analysis of twin supersonic plume resonance. *AIAA Paper* 87-2695.

Van Dyke, M. 1975 *Perturbation Methods in Fluid Mechanics* (revised annotated edn). Stanford, California: Parabolic Press.